

CHARACTERIZING MOTION CONTROL SYSTEMS TO ENABLE ACCURATE CONTINUOUS AND EVENT-BASED SCANS

J. Petersson*, T. Bögershausen, N. Holmberg, M. Olsson, F. Rojas, T. Richter
European Spallation Source ERIC, Lund, Sweden

Abstract

The European Spallation Source (ESS) is adopting innovative data acquisition and analysis methods using global timestamping for neutron scattering research. This study characterises the timing accuracy and reliability of the instrument control system by examining an integrated motion and fast detection system.

We designed an experimental apparatus featuring a motion axis controlled by a Beckhoff programmable logic controller (PLC) using TwinCAT 3 software. The encoder readback is timestamped in the PLC, which is time-synchronised with the ESS master clock via a Microresearch Finland event receiver (EVR) using Precision Time Protocol (PTP).

We repeatedly scanned the motor between known positions at different speeds. The system was characterised by correlating the position and timestamp recorded by the PLC with independent information using a fast optical position sensor read out directly by the MRF system.

The findings of this study provide a good benchmark for the upcoming experiments in neutron scattering research at ESS and should be interesting for those aiming to build similar setups.

INTRODUCTION

The European Spallation Source (ESS) is an international collaboration to build the world's most powerful neutron source [1]. Upon completion, it will produce a high-intensity proton beam, which will be directed onto a tungsten target, thereby generating neutrons through a process known as spallation. These neutrons can then be harnessed for a wide variety of scientific investigations, providing researchers with insights into the structural and dynamical properties of materials. Applications are broad and include fields such as solid-state physics, materials science, crystallography, biology, and archaeology.

To make the most out of this research potential, ESS employs a specific approach to handling the data produced. It captures neutron data in what is referred to as event mode: Each detected neutron is recorded individually and characterised by a timestamp and a pixel identifier, tracking the exact moment and location where the neutron hit the detector [2, 3]. Compared to histogram mode, where data is accumulated over a given period and represented as a set of counts, event mode retains more detailed information. This enhanced granularity of data provides researchers with the flexibility to bin and filter data in a resolution of their choosing, thus permitting more nuanced analyses.

To make the most out of the event mode recording, all relevant parameters about the measurement need to be known with the appropriate timing accuracy. Therefore, the timing system at ESS plays an integral part in the process by synchronising operations. It consists of an Event Generator (EVG) and a series of Event Receivers (EVRs) arranged in a tree topology to distribute events, clock signals, and data [4]. The EVG creates the event clock signal, which is transmitted to the EVRs. The EVRs, in turn, decode the incoming data and generate output triggers controlled by software. The EVRs can also handle inputs which can be timestamped. In addition to the timing system hardware, the Precision Time Protocol (PTP) is utilised to synchronise clocks, thus providing accurate timestamping and synchronisation among different subsystems.

In this paper, we investigate the correlation between motion data and event data within the ESS environment. The underlying question is: Given an event's timestamp, what is the uncertainty in position for a load mounted on the linear stage for that timestamp? By investigating this, we aim to quantify the performance of the motion control systems at ESS in terms of their ability to perform accurate continuous and event-based scans.

METHOD

In addition to the above-mentioned timing system, the experimental setup consists of a linear stage with a motor and encoder as well as a laser-based position detection system. A schematic overview is depicted in Fig. 1.

Laser System

A laser and a laser sensor are aligned on a beam table. The laser sensor (Thorlabs S120C) is connected to a power meter (Thorlabs PM100D) that delivers an analogue output voltage [5]. The output voltage is connected to a Schmitt trigger, which can deliver a 5V TTL pulse to the EVR for timestamping when the laser beam passes through the motorised aperture.

To characterise the optical detection, an LED triggered by the EVR was placed in front of the laser sensor to determine the time resolution of the laser readout system. The resolution of the laser timestamp setup is determined by triggering the LED with a TTL output from the EVR, which has an accurate timestamp, and then timestamp the TTL pulse generated from the laser sensor on an input on the EVR, effectively measuring the round-trip of the signal. The measured standard deviation of the round-trip time is on the order of 10 μ s, which is expected since the DC bandwidth of the sensor amplifier is 100 kHz.

* jonas.petersson@ess.eu

Content from this work may be used under the terms of the CC BY 4.0 licence (© 2023). Any distribution of this work must maintain attribution to the author(s), title of the work, publisher, and DOI

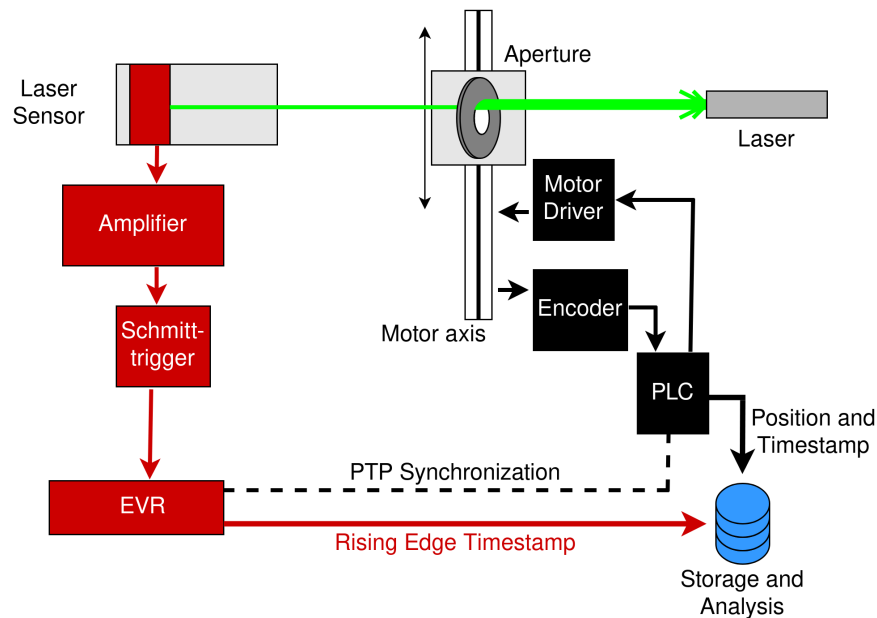


Figure 1: The setup consists of two subsystems that acquire timestamped data independently. The laser subsystem (red) consists of a laser sensor that is connected to an EVR, which timestamps rising edge events. The motor subsystem (black) consists of the PLC that controls the motor, reads the encoder position, and timestamps the encoder position. The PLC is time synchronised using PTP to the same clock as the EVR.

Motor System

The linear stage used for this test is a Huber Linear Stage 5101.10 [6]. The rated accuracy for the linear stage is $\pm 20 \mu\text{m}$ and the repeatability is $\pm 3 \mu\text{m}$. The motor is controlled via a Beckhoff PLC [7] that is time synchronised with PTP to the same clock as the EVR. The motor system features a stepper motor, which facilitates the movement of the axis. This stepper motor interfaces with an EtherCAT terminal integrated within the broader TwinCAT system [8]. The system oversees and manages the motor's operation using the numeric control function blocks. A notable feature is incorporating a control loop that dynamically adjusts the motor's velocity at intervals of 2 ms based on the encoder readings. The highest allowed velocity of the motor is 5 mm/s.

The PLC program reads the motor position and the associated timestamp at every 10 ms. This data is subsequently stored in dedicated data memory. An EPICS IOC retrieves this information over the network using a TCP/IP connection, specifically employing the PILS protocol [9] using ADS [10]. The EPICS records published are tagged with the original PLC timestamp.

Central to the facility's operation is the global facility time generated and governed by the MRF timing system. This critical time information is distributed into the PLC system using PTP. The Beckhoff distributed clock feature is active across the EtherCAT terminals, ensuring synchronised operations.

Initially, Network Time Protocol (NTP) was tested for time synchronisation. With a linear stage where the hard-

ware limit of the repeatability is around $6 \mu\text{m}$ and which is moving at 5 mm/s, the repeatability in terms of time would be 1.2 ms. In order for our timing system to allow this repeatability, NTP proved insufficient, and PTP is necessary to get synchronisation errors on the order of $10 \mu\text{s}$ instead of 10 ms.

Additional measures have been taken to verify the fidelity and accuracy of the timing and PTP subsystems. A precision, phase-locked 1Hz TTL hardware signal is generated in the EVR, which enables verification of the nanoseconds within each second. This provides a jitter measurement in the synchronisation, which can trigger an alarm. As an extra coarse safeguard, NTP can be used to ensure the epoch seconds.

Scan

The motor is scanned back and forth, driving the aperture across the laser's beam path, see Fig. 2. When the light detected by the laser sensor reaches a tunable threshold, a rising edge event is recorded in the EVR with a timestamp. This process involves only reasonably fast analogue electronics with a small and fixed latency. This provides fast detection of an (arbitrary) repeatable reference location for the motor.

By comparing the rising edge timestamps with the motor position readings provided by the encoder and their timestamps, the reported position of the motor at the time of the event can be inferred. By performing this measurement repeatedly, the accuracy of the timestamping, as the combined function of PTP synchronisation and application of the tim-

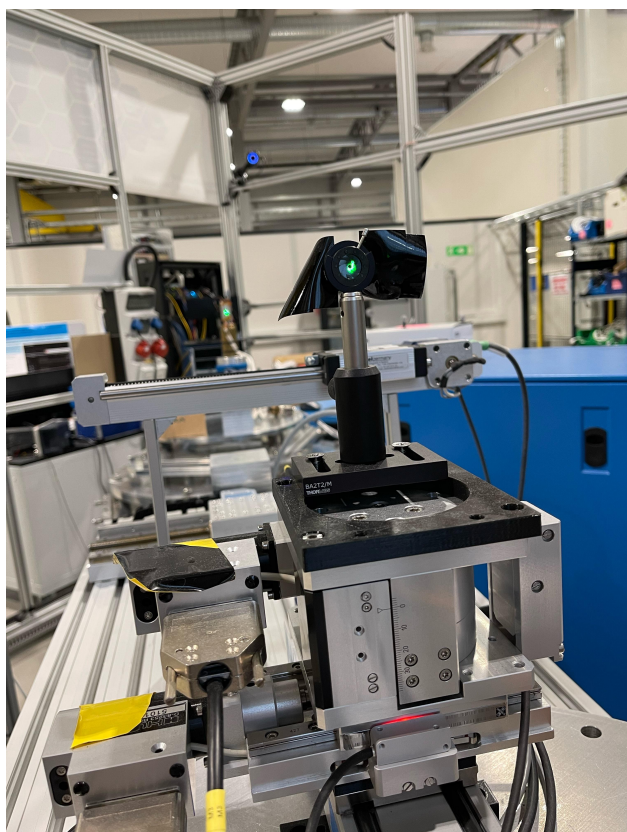


Figure 2: Photo of the laser shining on the aperture. The aperture is mounted on a three-axis linear stage platform where only the horizontal linear stage is scanned.

ing in the PLC, can be estimated quite accurately. This can also be expressed as a (speed-dependent) spatial uncertainty for the science use case.

A single measurement consisted of the aperture moving from the starting position to allow beam on the sensor, block the beam again and move back. This results in a single timestamp and corresponding encoder location reading. This was repeated 400 times at five different speeds each over the course of 23 hours.

RESULTS

In order to calculate the most accurate motor position at the time of the EVR event, the `interp1d` method in SciPy is used. An interpolation function is created using the motor timestamps and positions, and the interpolation function is then evaluated for the EVR timestamps, see Fig. 3. The interpolation assumes that the velocity is constant between the interpolated timestamps. Indeed, while the starting position of the aperture and motor has been varied in the measurements, care has been taken that any motor acceleration happens well before and after the rising edge reference location.

The effective encoder readings for the reference location are shown as a boxplot for each motor speed in Fig. 4. The box shows the lower and upper quartiles, the line represents the median, and the mean is the triangle. The highest

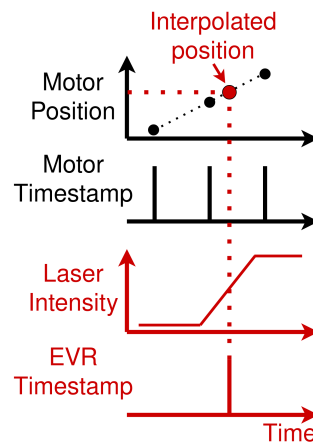


Figure 3: When the laser intensity crosses a threshold, a rising edge is sent to the EVR for timestamping (red graphs). The assumed motor position at this point in time is interpolated from the encoder positions reported at fixed intervals (black graphs).

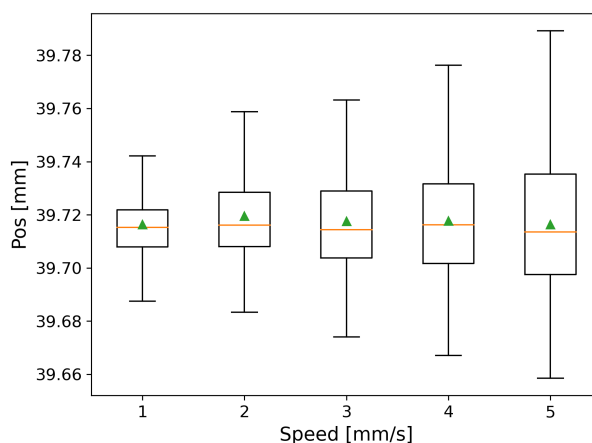


Figure 4: The interpolated motor positions are shown as a boxplot for each motor speed. The box shows the lower and upper quartiles, the line represents the median, and the mean is the triangle.

observed difference between interpolated positions for all speeds is 174.43 μm .

As expected, the positions' quartile width (as a measure of overall accuracy) increases with increasing motor speeds, see Fig. 4. However, the mean and average of the reported reference location are independent of the motor speed, and the quartiles' spread is symmetric. This indicates that there is no measurable latency in the time processing. The 10 μs noise measured when characterising the analogue processing should not be visible in the data, as the following estimation shows: With the highest velocity the motor is scanned at 5 mm/s, the timestamp error from the EVR and laser sensor might be 20 μs as a worst-case assumption. This corresponds to a motor position deviation on the order of $5 \text{ mm/s} \cdot 20 \mu\text{s} = 100 \text{ nm}$, which is well below the rated

repeatability of the linear stage of $\pm 3 \mu\text{m}$ and well below the discernible resolution of the y-axis in Fig. 4.

Instead, it can be assumed that the majority of the observed deviations and uncertainties exhibit the behaviour of a system governed by mechanical uncertainties. Also, in that case, larger deviations are expected at higher speeds. Due to the documented repeatability of the linear stage being $\pm 3 \mu\text{m}$, the best spread in the position we could expect would be on the order of $6 \mu\text{m}$. Since we have measured from $14 \mu\text{m}$ to $25 \mu\text{m}$ spread in position for the entire setup depending on the speed, it is close to the mechanical limits of the entire setup. In addition, vibrations in the workbench in Fig. 2 could affect the laser, sensor or aperture positions. Changes in the ambient light could also have an effect on the precision of the detection of the reference position, even though the laser is relatively powerful compared to the illumination.

CONCLUSIONS

This study has provided a characterisation of the motor accuracy within the instrument control system. The highest standard deviation of the interpolated motor position is on the order of $25 \mu\text{m}$ for this test equipment under specific conditions. A conclusion that likely can be transferred to similar setups is that time uncertainties are minor compared to mechanical effects, and a linear relationship was found between the standard deviation of the interpolated motor position and the motor speed. The speed-independent mean position indicates no significant latency in the timestamping process. This baseline is a practical reference for understanding the current capabilities of the motion control system.

The results of this investigation have two primary applications. Firstly, the findings inform instrument teams about the accuracy they can expect when conducting experiments. This information is essential for picking the correct components as well as planning and executing experiments, as it provides a clear understanding of the limitations and capabilities of the control system.

In addition, the results offer a benchmark that can be used to compare the performance of the motion system when upgrades or changes are made. This will help assess whether new components or software improve or degrade the system's performance. To this end, an automated test rig is being set up, where software updates can be evaluated prior to deployment. This allows us to track how incremental changes to software or hardware either improve or degrade the performance of the motion system in an easy way.

REFERENCES

- [1] ESS, <https://europeanspallationsource.se/>
- [2] M. Christensen *et al.*, "Software-based data acquisition and processing for neutron detectors at european spallation source—early experience from four detector designs", *J. Instrum.*, vol. 13, no. 11, T11002, 2018. doi:10.1088/1748-0221/13/11/T11002
- [3] A. Mukai *et al.*, "Architecture of the data aggregation and streaming system for the european spallation source neutron instrument suite", *J. Instrum.*, vol. 13, no. 10, p. T10001, 2018. doi:10.1088/1748-0221/13/10/T10001
- [4] J. C. Garcia, T. Korhonen, J. Lee, D. Piso, *et al.*, "Timing System at ESS", in *Proc. IPAC'17*, Copenhagen, Denmark, May 2017, pp. 4588–4590. doi:10.18429/JACoW-IPAC2017-THPVA064
- [5] Thorlabs, <https://www.thorlabs.com/>
- [6] Huber Linear Stage 5101.10, <https://www.xhuber.com/en/products/1-components/11-translation/linear-stage/510110/>
- [7] Beckhoff, <https://www.beckhoff.com/>
- [8] TwinCAT, <https://www.beckhoff.com/en-en/products/automation/twincat/>
- [9] PILS, <https://forge.frm2.tum.de/public/doc/plc/master/singlehtml/>
- [10] ADS, https://infosys.beckhoff.com/english.php?content=../content/1033/cx8190_hw/5091854987.html&id=